Supplementary materials and methods:

Fluorochrome-conjugated antibodies and flow cytometry

For flow cytometry analysis, PBMCs and skin dissociated cells were stained with fluorochrome-labeled monoclonal anti-human antibodies to CD8 (clone 3B5, Invitrogen), CD3 (clone UCHT1), CD4 (clone RPA-T4), CD2 (clone TS1/8), CD26 (clone BA5b) (all from Biolegend), CD7 (clone M-T701, BD Biosciences), and surface TCRVβ epitopes with the IOTest Beta Mark kit (Beckman Coulter, Indianapolis, IN). Data acquisition was done on LSRII and Fortessa flow cytometers (BD Biosciences). Flowjo X 10.0.7r2 was used for analysis.

Validation of inferred copy number variations (CNVs) by whole exome sequencing and methylation microarray:

Whole Exome Sequencing (WES) data from isolated malignant (CD4+TCRVβ1+) and non-malignant cells (CD8+ T cells) as well as single-cell RNA-seq (3P-single-cell RNA-sequencing kit V2; 10X Genomics) from PBMCs of an SS patient not otherwise included in the study was used to validate the inferred CNV profiles. WES data was pre-processed according to the GATK Best Practice Workflow guidelines (https://gatk.broadinstitute.org/hc/en-us/articles/360035535912-Data-pre-processing-for-variant-discovery) and CNVs were detected using two established pipelines: GATK Somatic copy number variant discovery (https://gatk.broadinstitute.org/hc/en-us/articles/360035535892-Somatic-copy-number-variant-discovery-CNVs-) and CNVkit [1] using default parameters. RNA expression from single cells were divided into malignant and non-malignant T cells based on overall expression patterns and distinct clustering. InferCNV was run with default parameters except for the cutoff which was set to 0.005 to include similar numbers of genes in the analysis as for the other samples in the study.

Copy number variation within malignant cells from the same SS patient was further verified by Infinium MethylationEPIC array (Illumina). CNV data was processed using the R packages 'minfi' and 'conumee' as described in the conumee vignette.

Validation of inferred CNVs using germline SNVs common between normal and malignant cells.

To identify germline mutations, variant calling was performed using HaplotypeCaller of the GATK v3.7 suite on malignant and two non-malignant clusters. The definition of the clusters are as follows - 1) malignant cells: cells with the highest CDR3 sequence frequency for TCR β, 2) polyclonal cells: all CD3+CD4+ T cells that do not possess the malignant clonotype, 3) remaining cells: barcodes not belonging to cluster 1 or 2. Cell barcodes of the clusters were used to demultiplex the BAM file. BAM files were pre-processed and VCFs were generated according to the GATK Best Practice Workflow for RNA-seq (https://gatk.broadinstitute.org/hc/en-us/articles/360035531192-RNAseq-short-variant-discovery-SNPs-Indels-). We then identified bi-allelic SNVs from the VCF, and excluded SNVs spanning the X and Y chromosome, as well as those found within all HLA genes. Only SNVs with a minimum read depth of 50 UMIs for each of the 3 clusters were included. To identify heterozygous genotypes, we use the UMI depth, N, and major allele frequency, k, and tested it against a heterozygous null model (defined as a Binomial distribution, parameterized with Psuccess = 0.5). Heterozygous SNVs were selected if their variant allele frequency from both the polyclonal and remaining cell clusters did not reject the null hypothesis ($P >= 0.05$). Finally, p-values were generated for each heterozygous SNVs from allele frequencies in the malignant cluster by testing it against the same heterozygous null model. The significance threshold was set at $p < 5.0 \times 10\text{-}8$.

Comparison of CNV profiles using copyKAT

The InferCNV profile from CTCL patient SS1 was compared to results using copyKAT, an additional method of inferring CNV states from scRNA-seq data, as previously described.[2]

Additional phylogenetic methods

From the copy number profiles derived from InferCNV HMM results, we constructed additional phylogenetic trees using Minimum Evolution and Average Linkage (UPGMA) with R package ape v5.3. Minimum evolution finds trees with the least amount of summed up branch lengths. ME's objective is similar to the maximum parisomy (MP) approach, but uses distances rather than sequences. Unlike neighbor-joining, UPGMA assumes constant mutation rates. For each tree, bootstrap analysis of a 100 replicates was performed each time. Visualization of the phylograms were constructed using R package ggtree v2.0.1.

Cell cycle analysis

Cell cycle scoring of skin- and blood-derived malignant T cells was done as described on the Seurat cell-cycle scoring and regression vignette (https://satijalab.org/seurat/archive/v3.0/cell_cycle_vignette.html). This utilizes a list of canonical markers delineating G1, S and G2/M phases and is based on the scoring strategy described in Tirosh *et al*., 2016.[3] Scores were superimposed on transcriptional trajectories using Monocle 2 v2.14[4] of malignant T cells from five CTCL patients.

Supplementary tables:

Volunteer ID	Sex	Age	Disease Stage at diagnosis (TNMB)	Disease Stage and burden at collection (TNMB)	SS or MF category	CD4/ CD8 ratio	Phenotypically malignant cells out of all CD4+ T cells in blood	Clonal malignant TRAV and TRBV genes	Skin lesions	Therapies 2 weeks prior to collection?	Past therapies for lymphoma	Symptoms history and disease onset
CTRL-1	M	41	N/A	N/A	N/A	0.6:1	N/A	N/A	N/A	N/A	N/A	N/A
SS1	F	49	T4N3M1B2	T4N3M1B2	SS, stage IVb	5:1	60%	TRAV 3, TRBV 12-3	< 1% TBSA, patches (suspect invisible erythroderma)	No	No previous therapies	Developed rash 6 months before diagnosis. Tissue collected at diagnosis.
SS2	M	62	T4NxM0B2	T4NxM0B2	SS, stage IVa1	2:1	17%	TRAV 9-2, TRBV 5-4	Erythroderma	No	Topical-Clobetasol	Developed erythroderma a year before diagnosis. Tissue collected 2 months after diagnosis.
SS3	F	71	T4NxM0B2	T4NxM0B2	SS, stage IVa1	-	21%	TRAV 22, TRBV 5-6	Plaques/rashes	No	No previous therapies	Developed rash 1 year before diagnosis. Tissue collected 1 month after diagnosis.
SS4	M	56	T4N3M1B2	T4N3M1B2.	SS, stage IVa2	3:1	36%	TRAV 35, TRBV 3-1	Erythroderma	No	Topical-targretin, bexarotene fluocinolone, betamethasone	Developed itchy rash a year before diagnosis. Tissue collected at diagnosis
MFIV1	F	39	T2N0M0B0	T2N1M1B0	MF, stage IVb (advanced from MF stage Ib)	1.1:1	35.8%	TRAV 35, TRBV 20-1	Plaques	No	Systemic-methotrexate, interferon, romidepsin	Developed skin macules 3 years preceding MF stage 1b diagnosis. Advanced to MF stage IVB 2 years and 4 months after. Tissue collected 2 weeks after advancing.
SS5	F	71	T2N0M0B0	T1aN0M0B2	SS, stage IVa1 (advanced from MF stage Ib)	9:1	60%	TRAV 1-1, TRBV 6-5	85% TBSA, Erythroderma	Extracorporeal photophoresis	Systemic-extracorporeal photophoresis, Topical-Taxotere, Adriamycin and Cyclophosphamide	Blanching erythematous rashes 6 months before MF stage 1b diagnosis. Advanced to SS during ECP treatment 4 years after. Tissue collected 1 year after advancing to SS
SS6	M	78	T4N3M0B1	T4N3M0B1	SS, Stage IVa2	4:1	46%	TRAV 8-4 , TRBV 6-5	100% TBSA, erythroderma	No	No previous therapies for lymphoma	History of red, itchy rashes for over 15 years. Tissue collected 1 month after diagnosis.

Supplementary Table 1. Clinical notes and data of CTCL patients and a healthy control. TBSA: total body surface area.

Phenotypically malignant cells were defined as CD7- and CD26- CD4+ T cells or clonally expanded CD4+ T cells based on TCRvB staining that were also CD7- and CD26-.

Biospecimen ID	*M*	*T4N*	*T8N*	*T4M*	*T8M*	*T8E*	*gdT*	*NK*	*BC*	*BCM*	*MO*	*DC*	*pDC*	*FB*	*KRT*	*UNC*
SS1 blood	0.44	0.18	0.03	0.10	0.03	0.05	0.00	0.06	0.06	0.01	0.02	0.00	0.00	0.00	0.00	0.01
SS2 blood	0.09	0.00	0.00	0.05	0.01	0.08	0.02	0.05	0.03	0.00	0.59	0.01	0.00	0.00	0.00	0.07
SS3 blood	0.49	0.13	0.00	0.04	0.00	0.05	0.00	0.00	0.03	0.00	0.25	0.00	0.00	0.00	0.00	0.01
SS4 blood	0.14	0.00	0.00	0.26	0.12	0.05	0.00	0.20	0.14	0.00	0.06	0.00	0.01	0.00	0.00	0.01
MFIV1 blood	0.28	0.09	0.06	0.15	0.01	0.23	0.00	0.14	0.02	0.00	0.00	0.01	0.00	0.00	0.00	0.01
SS5 blood	0.21	0.00	0.00	0.23	0.02	0.01	0.01	0.18	0.21	0.00	0.08	0.00	0.00	0.00	0.00	0.04
SS6 blood	0.37	0.13	0.00	0.17	0.13	0.00	0.00	0.03	0.06	0.00	0.11	0.01	0.00	0.00	0.00	0.00
HC1 blood	0.00	0.08	0.14	0.14	0.14	0.08	0.03	0.05	0.07	0.02	0.21	0.03	0.01	0.00	0.00	0.02

Supplementary Table 2. Fractions of PBMC populations making up the blood of CTCL patients. M: Malignant T cells, **T4N**: Naïve CD4+ T cells, **T8N**: Naïve CD8+ T cells, **T4M**: Memory CD4+ T cells, **T8M**: Memory CD8+ T cells, **T8E**: Effector CD8+ T cells, **gdT**: γ/δ T cells, **NK**: Natural killer cells, **BC**: B cells, **BCM**: Memory B cells, **MO**: Monocytes/macrophages, **DC**: Dendritic cells, **pDC**: plasmacytoid dendritic cells, **FB**: Fibroblasts, **KRT**: Keratinocytes, **UNC**: Unclassified. Apoptotic keratinocytes are filtered out.

Biospecimen ID	*M*	*T4N*	*T8N*	*T4M*	*T8M*	*T8E*	*gdT*	*NK*	*BC*	*BCM*	*MO*	*DC*	*pDC*	*FB*	*KRT*	*UNC*
	0.16	0.00	0.00	0.002	0.10	0.00	0.00	0.0	0.00	0.000	0.0	0.04	0.0000	0.0	0.59	0.00
SS1 skin	80	81	00	0	73	00	00	020	00	0	445	05		324	31	20
	0.02	0.00	0.00	0.138	0.36	0.16	0.00	0.0	0.02	0.000	0.0	0.15	0.0040	0.0	0.00	0.01
SS2 skin	78	00	00	9	51	67	79	833	38	0	159	08		000	00	59
	0.17	0.00	0.00	0.004	0.00	0.00	0.00	0.0	0.00	0.000	0.2	0.19	0.0000	0.1	0.20	0.00
SS3 skin	95	64	00	3	00	43	00	000	00	0	863	23		197	73	00
	0.52	0.00	0.00	0.028	0.04	0.00	0.00	0.0	0.01	0.000	0.0	0.08	0.0000	0.0	0.23	0.00
SS4 skin	63	00	00	7	78	48	00	287	91	0	191	37		000	92	24
	0.28	0.00	0.00	0.000	0.00	0.00	0.00	0.0	0.00	0.000	0.2	0.30	0.0000	0.1	0.06	0.00
MFIV1 skin	65	00	00	0	00	00	00	000	00	0	066	30		295	61	83
	0.00	0.00	0.02	0.040	0.02	0.04	0.00	0.0	0.00	0.040	0.0	0.14	0.0000	0.0	0.00	0.66
HC1 skin	00	00	00	0	00	00	00	400	00	0	000	00		000	00	00

Supplementary Table 3. Fractions of tissue dissociated populations making up the skin of CTCL patients. M: Malignant T cells, **T4N**: Naïve CD4+ T cells, **T8N**: Naïve CD8+ T cells, **T4M**: Memory CD4+ T cells, **T8M**: Memory CD8+ T cells, **T8E**: Effector CD8+ T cells, **gdT**: γ/δ T cells, **NK**: Natural killer cells, **BC**: B cells, **BCM**: Memory B cells, **MO**: Monocytes/macrophages, **DC**: Dendritic cells, **pDC**: plasmacytoid dendritic cells, **FB**: Fibroblasts, **KRT**: Keratinocytes, **UNC**: Unclassified. Apoptotic keratinocytes are filtered out.

Target	Clone	Barcode	Concentration (ug/ml)
CD3	UCHT1	TAGAACCGTATCCGT	5
CD4	RPA-T4	TGTGGTAGCCCTTGT	5
CD8	RPA-T8	TATCCCTGCCTTGCA	5
TCRb	IP26	TAGCAGTCACTCCTA	5
TCRg	B1	CTATCGTTTGATGCA	5
CD44	BJ18	ATCTGTATGTCACAG	0.5
CD62L	DREG-56	AACCGCGCTTCAGAT	5
Ox40 (CD134)	Ber-ACT35 (ACT35)	GCGATTCATGTCACG	5
B7-H1 (PD-L1)	29E.2A3	GTTGTCCGACAATAC	5
EpCAM (CD326)	9C4	AAACTCAGGTCCTTC	5
CD66b	6/40c	GCGAGAAATCTGCAT	5
MHCII (HLA-DR)	L243	GCCTAGTTTGAACGC	5
CD45	HI30	CGATTTGATCTGCCT	0.5
CD19	HIB19	TCACGCAGTCCTCAA	5
B220 (CD45R)	RA3-6B2	GTATAGACCAAAGCC	5
CD11c	3.9	CGTATGCCCTTTAGA	5
CD14	M5E2	GCTTGGGCAATTAAG	5
CD34	581	TGGCTTAGCTTTACA	5
CD56	5.1H11	CGTATCTGTCATTAG	5
CD16	B73.1	TATATCCCTCAACGC	5
CD2	TS1/8	AATTCCGTCAGATGA	1
CD5	UCHT2	ATTCCTCATTCCTGA	5
CD45RA (Biolegend TotalSeq-C)*	HI100	TCAATCCTTCCGCTT	1.25
CD45RO (Biolegend TotalSeq-C)*	UCHL1	CTCCGAATCATGTTG	1.25
CCR7	G043H7	ACTGCCATATCCCTA	5
CD11b	ICRF44	CCATTCATTTGTGGC	5
CD1a	HI149	CAACTTGGCCGAATC	5
CD27	M-T271	ACGCAGTATTTCCGA	5
CD69	FN50	CATTAGAGTCTGCCA	5
PECAM (CD31)	WM59	CTCAGCCCTAGTATA	5
CD138	DL-101	CTCGTTTGTAGCAAT	5
CD24	ML5	GATTCCTTTACGAGC	5
Siglec-8	7C9	GAACCGTACCCATGA	5
LAMP1	H4A3	GAGAAATCAACCAAG	5
C-kit (CD117)	104D2	CTTACCTAGTCATTC	5
IL7Ralpha (CD127)	A019D5	TTGTTGTATCCGATC	5

CTLA4	BNI3	CAGAGCACCCATTAA	5
HLA-A,B,C	W6/32	GGATGTACCGCGTAT	5
CD77	5B5	GTCATTGTATGTCTG	5
CD366 (tim3)	F38-2E2	GGGCAATTAGCGAGT	5
CD223 (lag3)	11C3C65	GCCATTCCTGCCTAA	5
CD28	CD28.2	GACAGTCGATGCAAC	5
CD7	CD7-6B7	CTCCCTAGTTCCTTT	5
CD26 (Adenosine)	BA5b	TTCCTGCACGAGGAT	5
PD-1 (CD279)	NAT105	GTTGGATGGTAGACT	5
PD-L1 (CD274)	MIH1	GCAGTTGTCCGATTC	5
IgG1	MOPC-21	GCGCAACTTGATGAT	5
IgG2a	MOPC-173	TCCCTTGCGATTTAC	5
CD123*	9F5	TTAACCAGTTGTACC	5
CD25*	M-A251	TGACCCTATTGAGAA	5
B7-1*	2D10	ACGAATCAATCTGTG	5
B7-2 (CD86)*	IT2.2	GTCTTTGTCAGTGCA	5
CD40*	5C3	CTCAGATGGAGTATG	5
CD40L*	24-31	GCTAGATAGATGCAA	5
CLA*	HECA-452	TCATCGTTTGTTCCT	5
CD14 (Biolegend TotalSeq-C)**	M5E2	TCTCAGACCTCCGTA	1
CD56 (Biolegend TotalSeq-C)**	5.1H11	TCCTTTCCTGATAGG	1
CD28 (Biolegend TotalSeq-C)**	CD28.2	TGAGAACGACCCTAA	1.25
CD69 (Biolegend TotalSeq-C)**	FN50	GTCTCTTGGCTTAAA	0.625

Supplementary Table 4. Human ADT targets and barcodes.

*These antibodies were only used for SS2-SS6.

**These Biolegend TotalSeq-C antibodies were only used for SS3 and SS4 instead of their "home-conjugated" counterparts.

Supplementary figures:

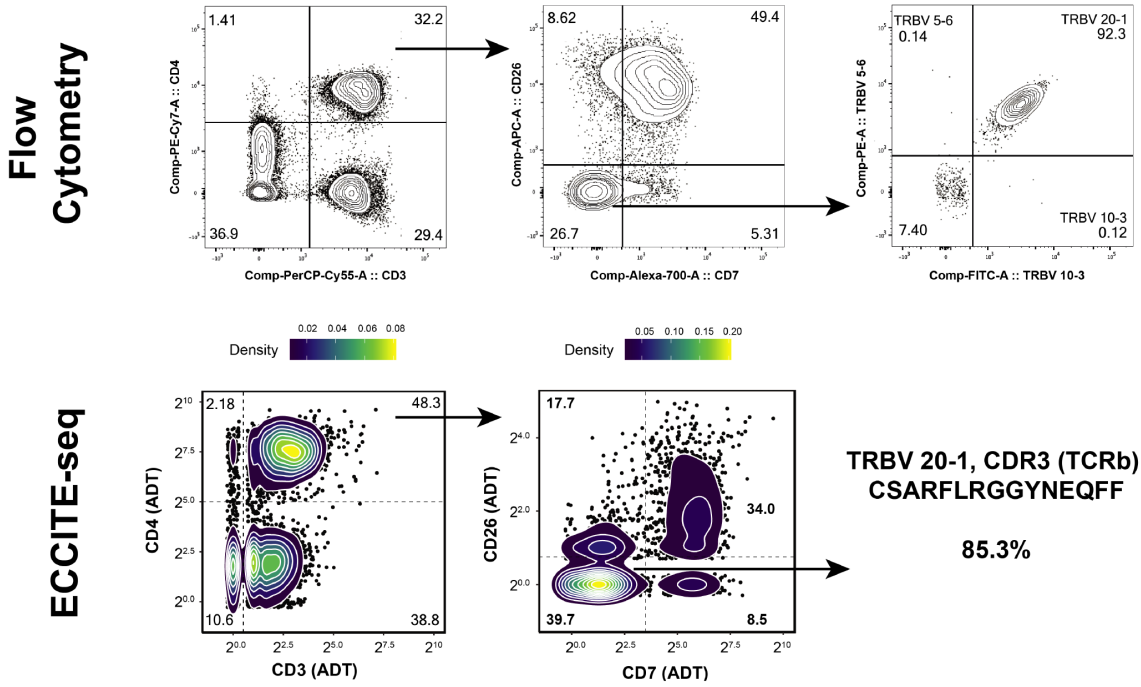

Supplementary Figure 1. Analysis based on ADT counts recapitulates data from FACS analysis. Digital rendering of ADT counts from patient MFIV1 for markers commonly used for flow cytometric analysis of patient blood (CD3, CD4, CD7, and CD26) largely recapitulates the distribution of cells within the gates/quadrants outlined in the FACS analysis of the same patient. Majority of the malignant clone (as evidenced by TCR clonotype revealed in ECCITE-seq analysis) falls into the Q4 quadrant with characteristic loss of CD26 and CD7.

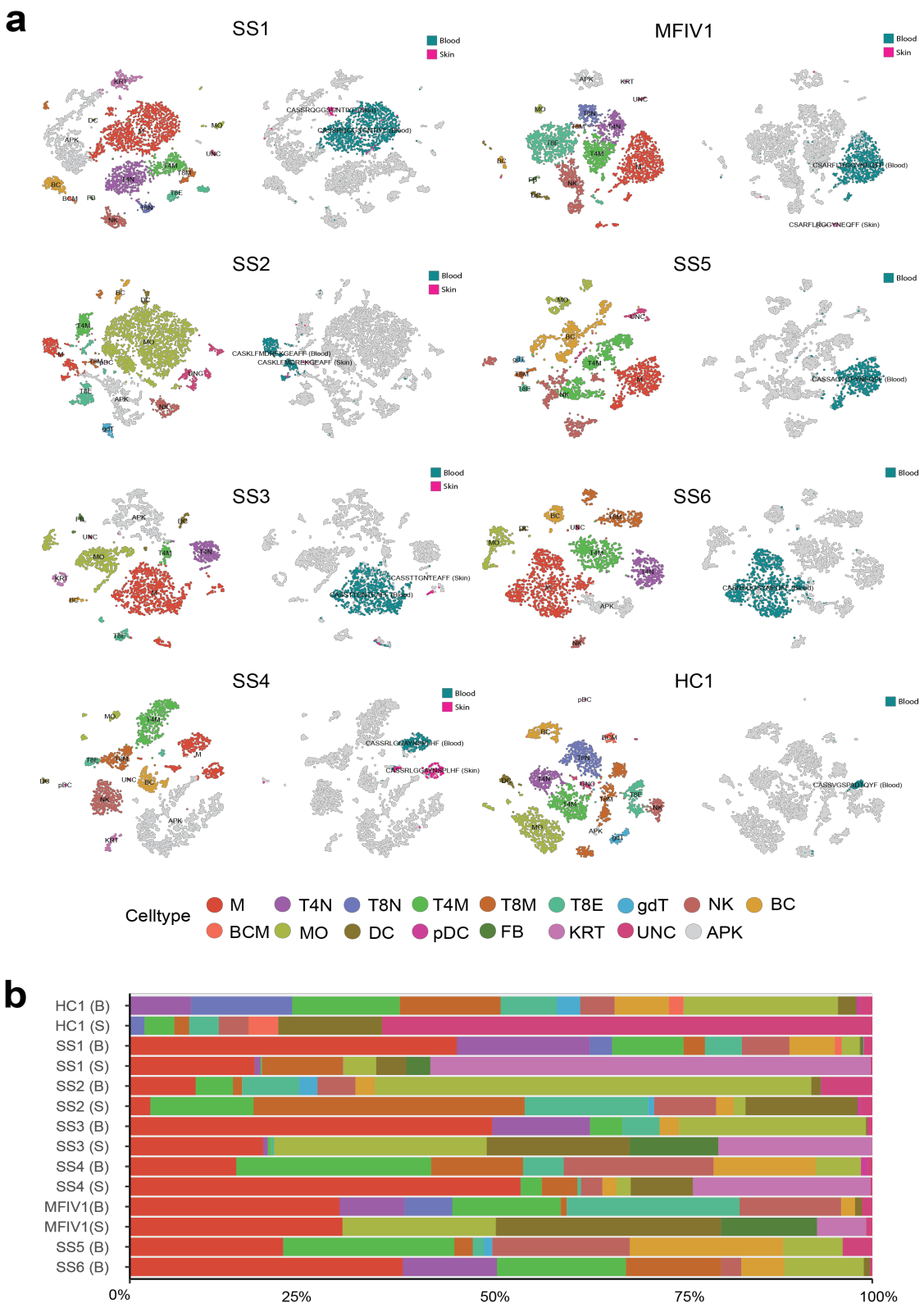

Supplementary Figure 2: t-SNE plots of 7 CTCL patients and 1 healthy control. a, t-SNE plots of single cells from PBMCs and skin dissociated tissue of a healthy control and 5 CTCL patients (SS1-MFIV1) and PBMCs only of 2 CTCL patients (SS5 and SS6) clustered by GEX and ADT multimodal WNN analysis. Different immune populations are colored and visualized based on their GEX and ADT profile (left). TCR β chain monoclonal cells are visualized (right) and colored by their tissue of distribution. Interestingly, one patient (SS2) had a mixture of malignant T cells expressing

β chain CDR3 but one of two different TCR α chain CDR3 sequences sharing the same TCR α chain variable region gene. **b,** Bar plot showing distribution of populations in tissues of each donor. **M**: Malignant T cells, **T4N**: Naïve CD4+ T cells, **T8N**: Naïve CD8+ T cells, **T4M**: Memory CD4+ T cells, **T8M**: Memory CD8+ T cells, **T8E**: Effector CD8+ T cells, **gdT**: γ/δ T cells, **NK**: Natural killer cells, **BC**: B cells, **BCM**: Memory B cells, **MO**: Monocytes/macrophages, **DC**: Dendritic cells, **pDC**: plasmacytoid dendritic cells, **FB**: Fibroblasts, **KRT**: Keratinocytes, **APK**: Apoptotic keratinocytes, **UNC**: unclassified.

a

Clonotype Identity associated with top TCRβ

HC1

TCRα: CAASWSPLGGSARQLTF
TCRβ: CASSVGSPADTQYF
(n = 92)

SS1

TCRα: CAGSLYNFNKFYF
TCRβ: CASSRQGGSGNTIYF
(n = 1634)

SS2

TCRα: CALRKRGNTPLVF
TCRβ: CASKLFMDREKGEAFF
(n = 278)

SS3

TCRα: CAFPPGPNNAGNMLTF
TCRβ: CASSTTGNTEAFF
(n = 766)

b

t-SNE of Top 5 Clonotypes Highlighted

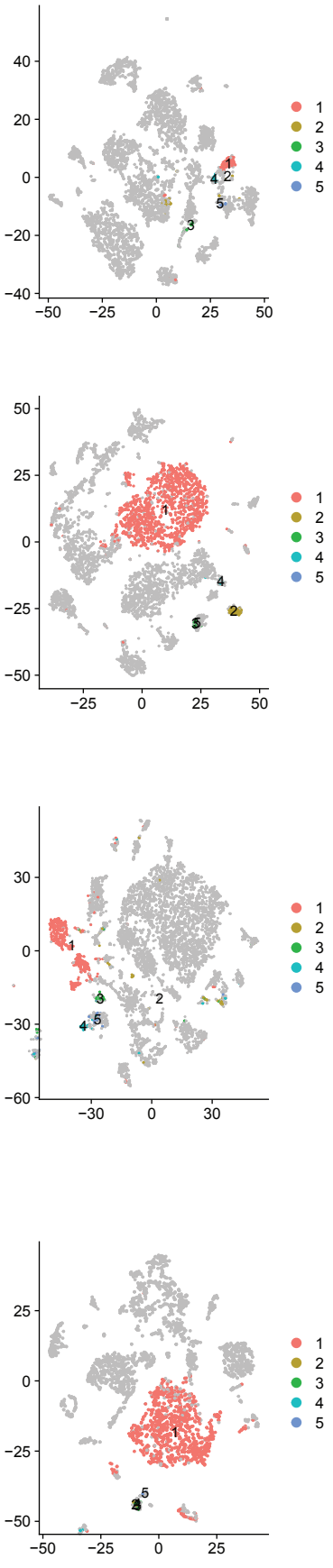

c

Gene Expression Levels of CTCL Markers for Top 5 Clonotypes

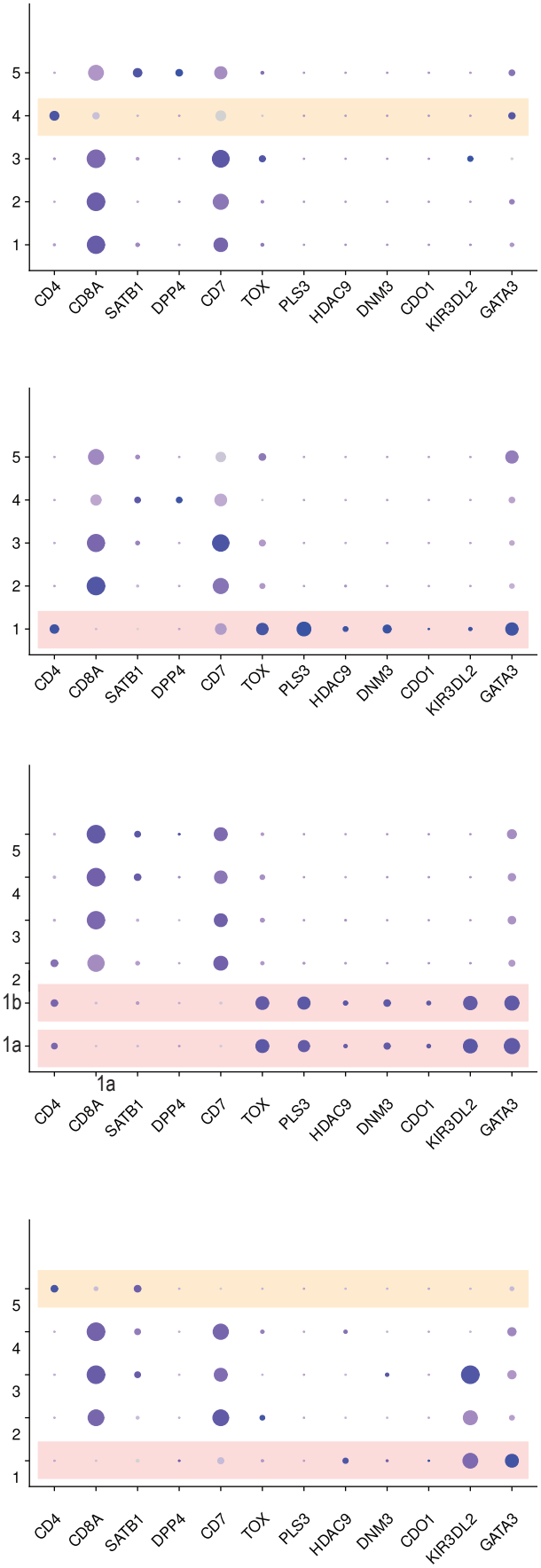

Supplementary Figure 3: Definition of malignant clone in the skin and blood of a HC and CTCL patients (HC1-SS3) based on CDR3 identity and gene expression patterns. a, Clonotype identities associated with the highest frequency TCR β CDR3 expressing T cells in donors HC1-SS3. **b,** GEX and ADT based t-SNE plots showing the top 5 clonotypes for each donor based on unique expression of TCR β CDR3s. Interestingly, patient SS2 possessed two clonotype identities in the highest frequency clonotype/malignant T cell cluster sharing an identical TCR β CDR3 but each one of two different TCR α chain CDR3 sequences sharing the same TCR α chain variable region gene (1a: CALRKRGNTPLVF, n = 278; and 1b: CHGSSNTGKLIF). c, Dot plots showing expression of CD4, CD8A, and common SS/CTCL markers used to identify malignant T cells across the top 5 clonotypes of each donor. The top clonotype/malignant clone in each patient is highlighted in pink shade, clonotypes consisting of CD4+ T cells are highlighted in beige shade, and clonotypes consisting of CD8+ T cells are unshaded.

a

Clonotype Identity associated with top TCRβ

b

t-SNE of Top 5 Clonotypes Highlighted

c

Gene Expression Levels of CTCL Markers for Top 5 Clonotypes

SS4

TCRα: CALVNAGNNRKLIW
TCRβ: CASSRLGGAYNSPLHF
(n = 211)

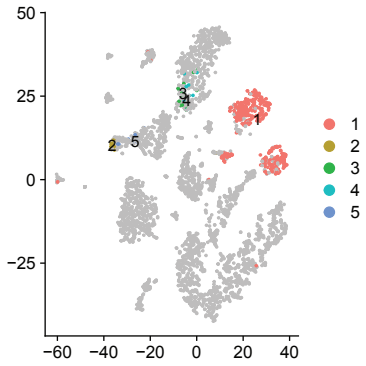

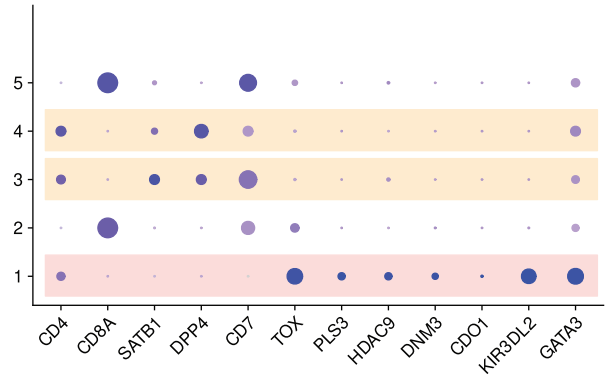

MFIV1

TCRα: CAGQLRNAGGTSYGKLTF
TCRβ: CSARFLRGGYNEQFF
(n = 564)

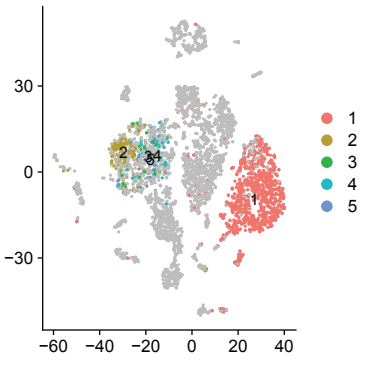

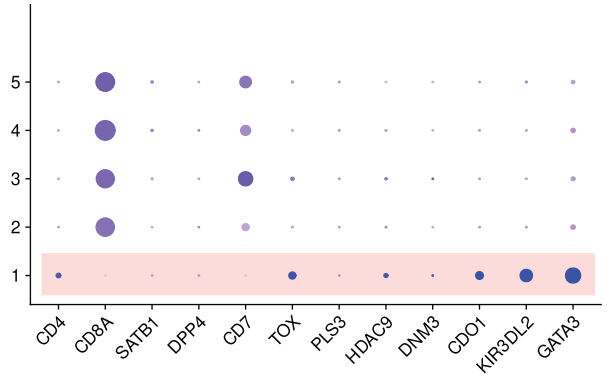

SS5

TCRα: CAVRAPNTGGFKTIF
TCRβ: CASSAGVGPYNEQFF
(n = 702)

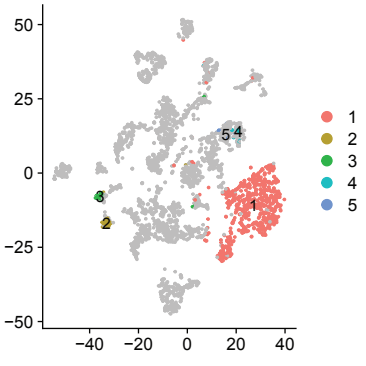

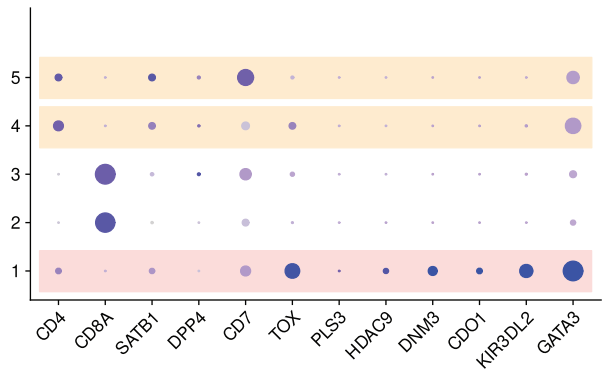

SS6

TCRα: CAGKRDDKIIF
TCRβ: CASRSQGSYNEQFF
(n = 938)

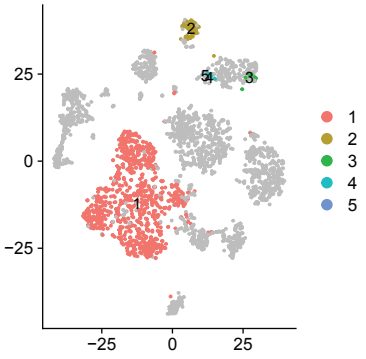

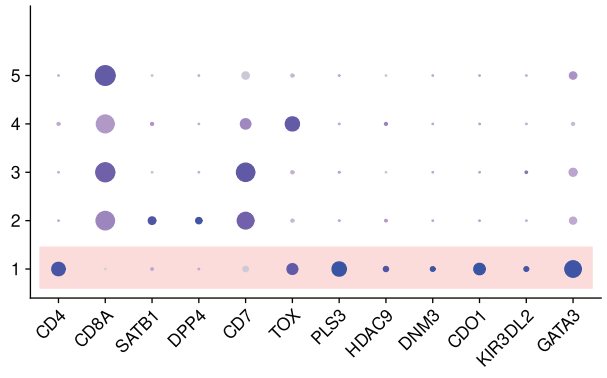

Supplementary Figure 4: Definition of malignant clone in the skin and blood of CTCL patients (SS4-SS6) based on CDR3 identity and gene expression patterns.

Clonotype identities associated with the highest frequency TCR β CDR3 expressing T cells in donors SS4-SS6. **b,** GEX and ADT based t-SNE plots showing the top 5 clonotypes for each donor based on unique expression of TCR β CDR3s. **c,** Dot plots showing expression of CD4, CD8A, and common SS/CTCL markers used to identify malignant T cells across the top 5 clonotypes of each donor. The top clonotype/malignant clone in each patient is highlighted in pink shade, clonotypes consisting of CD4+ T cells are highlighted in beige shade, and clonotypes consisting of CD8+ T cells are unshaded.

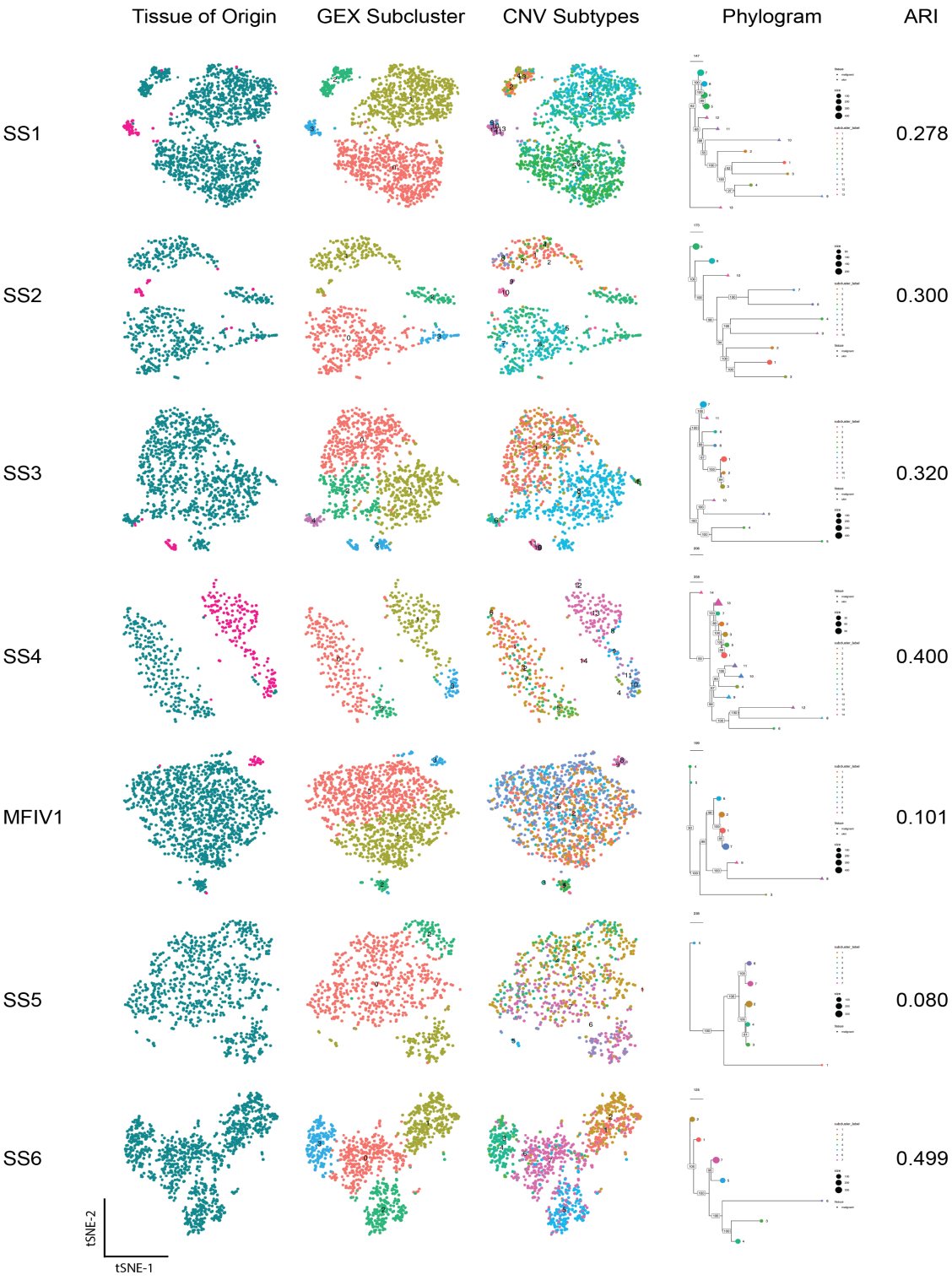

Supplementary Figure 5: Concordance between GEX sub-cluster groupings and inferred CNV sub-clonal groupings of patient derived malignant T cells. Malignant T cells from skin and blood of five CTCL patients (SS1-MFIV1) and blood only of two CTCL patients

(SS6 and SS7) are clustered by GEX and visualized by tissue of origin, GEX sub-clusters and CNV sub-clones (left to right). Phylograms of malignant T cells from each patient bootstrapped 100 times and rooted using their non-malignant polyclonal T cells show malignant evolution of CNV defined clusters. The Adjusted Rand Index (ARI) is used to determine cluster alignment between GEX-defined sub-clusters and CNV-defined sub-clones.

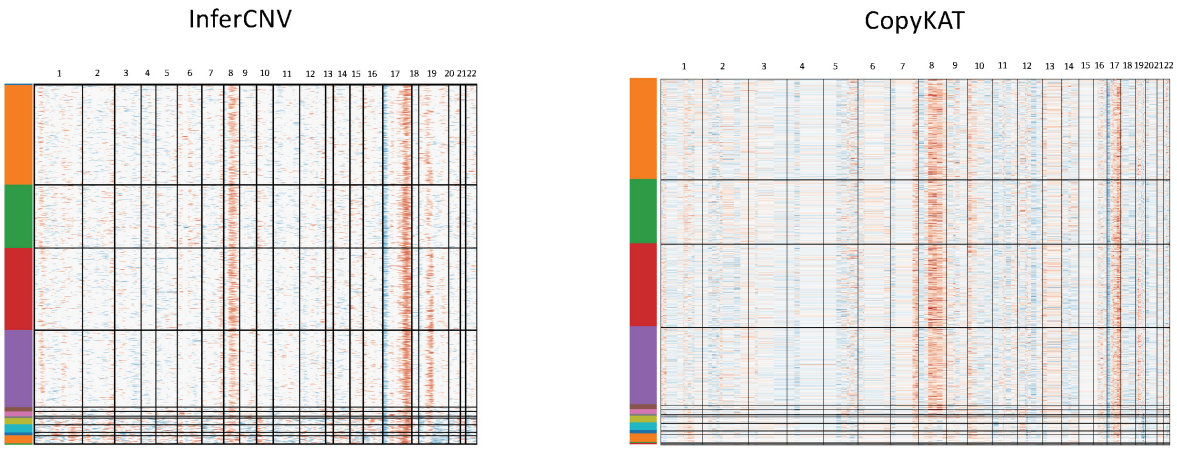

Supplementary Figure 6. CNV profiling of blood-derived malignant T cells from an SS patient using InferCNV and CopyKAT. Plots showing gain (in red) and loss (in blue) inferred genomic events in a patient with maximal transcriptional heterogeneity (SS1). Sub-clonal populations are colored by CNV profiling. CNV events in chromosomes, labeled from left to right (1-22), are largely recapitulated between InferCNV and CopyKAT, an alternative method of CNV profiling from scRNA-seq data.[2]

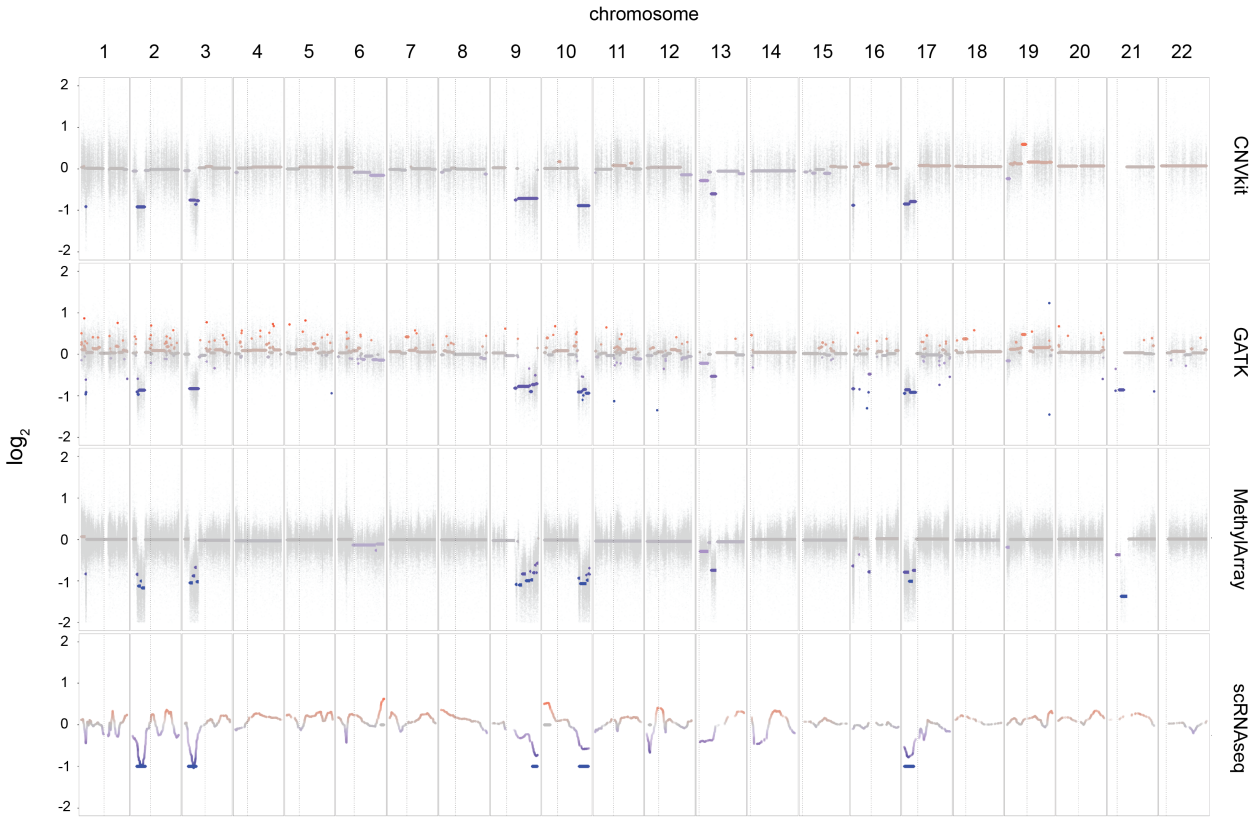

Supplementary Figure 7: Validation of inferred CNVs from scRNA-seq using whole exome sequencing and methylation microarray. Plots showing gain (in red) and loss (in blue) events in malignant T cells from the blood of a CTCL patient (independent SS patient) from whole exome sequencing and scRNA-seq. Two methods of analysis from whole exome sequencing (top 2 rows) and one from methylation microarray analysis (3rd row) were used to compare to inferred CNV analysis from scRNA-seq (bottom row) on the same patient.

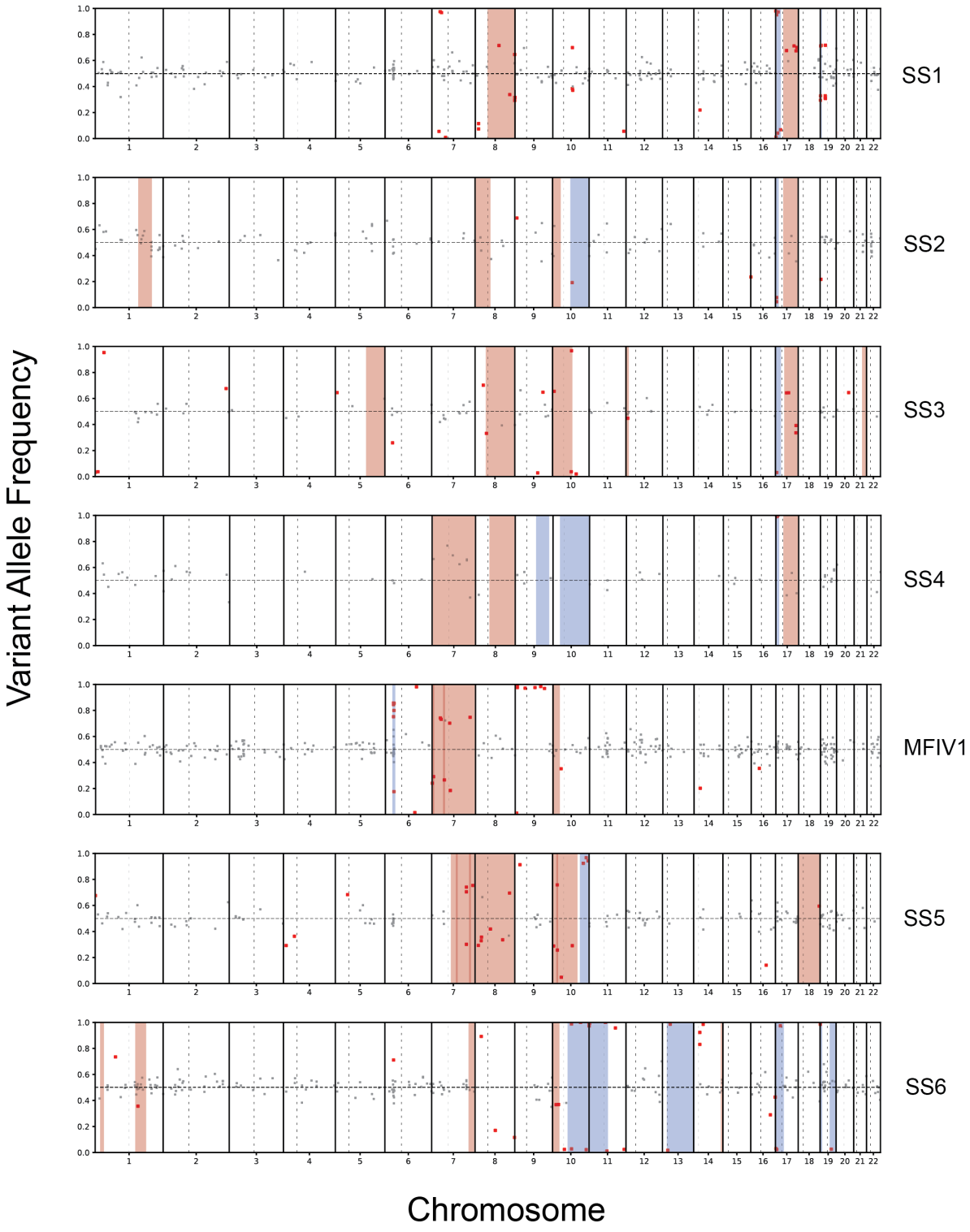

Supplementary Figure 8: Validation of inferred CNVs using germline SNVs common between normal and malignant cells. During LOH or insertion events, variant allele

frequencies of common heterozygous SNVs deviate from their expected allele frequencies. A Manhattan plot of $-\log_{10}$ transformed *p*-values depict SNVs that reject the null hypothesis (red points) generally overlap scRNA-seq inferred CNVs: insertion (red) or deletion (blue). Variant allele frequency (N, k) are tested against a heterozygous null model ($P_{success} = 0.5$, Binomial distribution). Genome-wide significance threshold is set at $p < 5.0 \times 10^{-8}$.

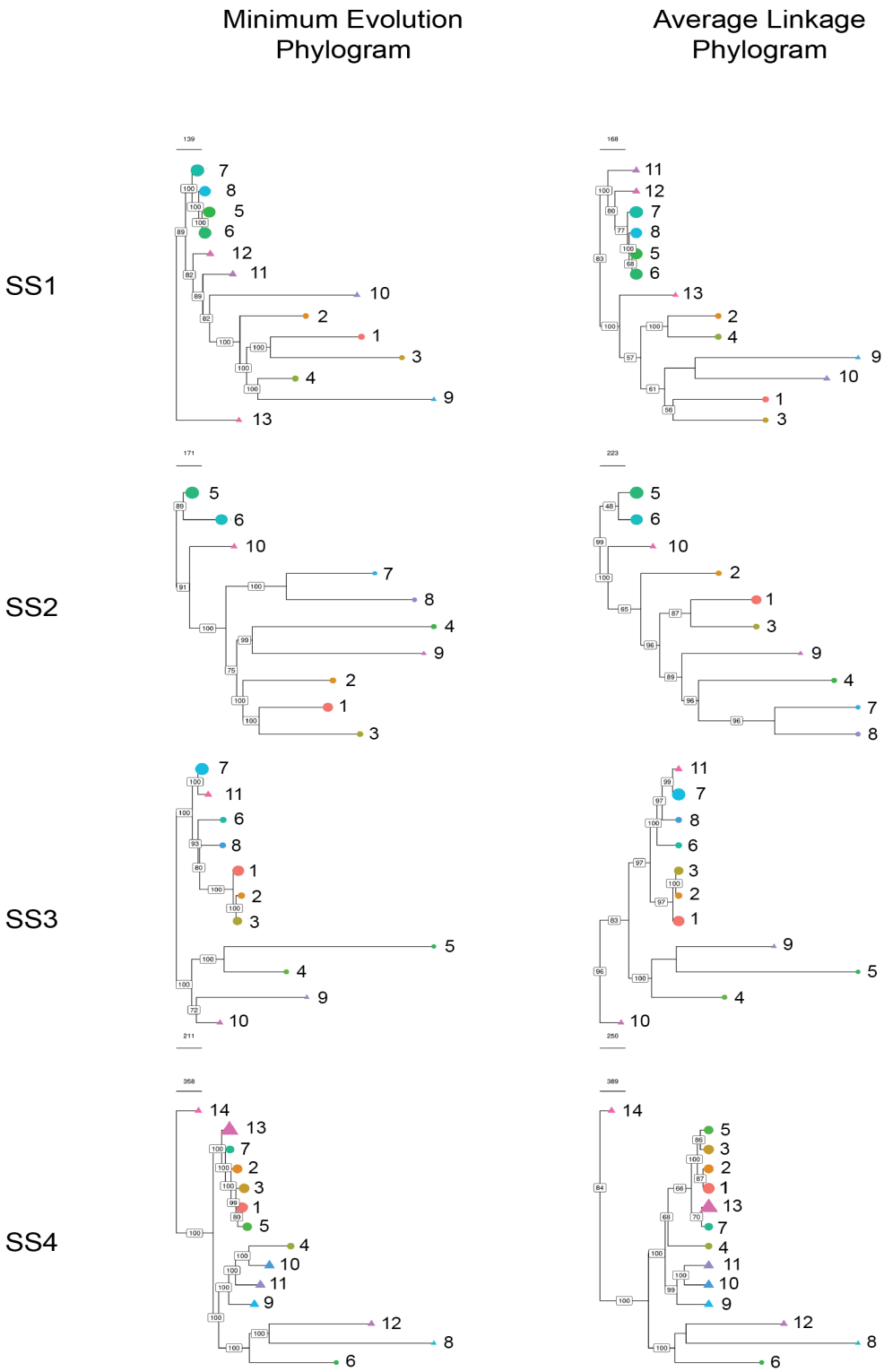

Supplementary Figure 9. Comparison of different phylogram building methods on patient skin- and blood-derived malignant T cells. Phylograms of malignant T cells from each

CTCL patient (SS1-SS4) rooted using their non-malignant polyclonal T cells show malignant evolution of CNV defined clusters across multiple platforms.

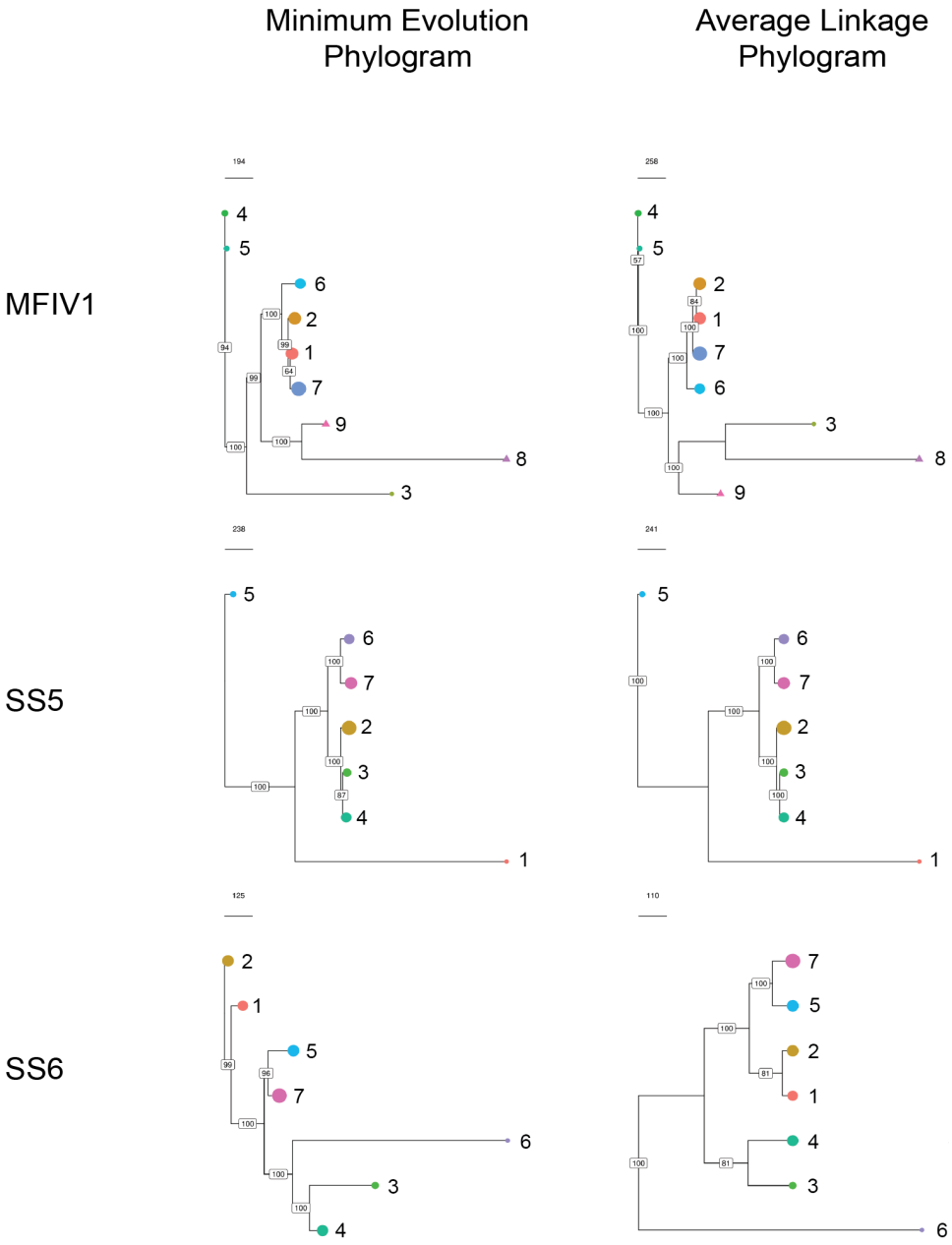

Supplementary Figure 10. Comparison of different phylogram building methods on patient skin- and blood derived malignant T cells. Phylograms of malignant T cells from each CTCL patient (MFIV1-SS6) rooted using their non-malignant polyclonal T cells show malignant evolution of CNV defined clusters across multiple platforms.

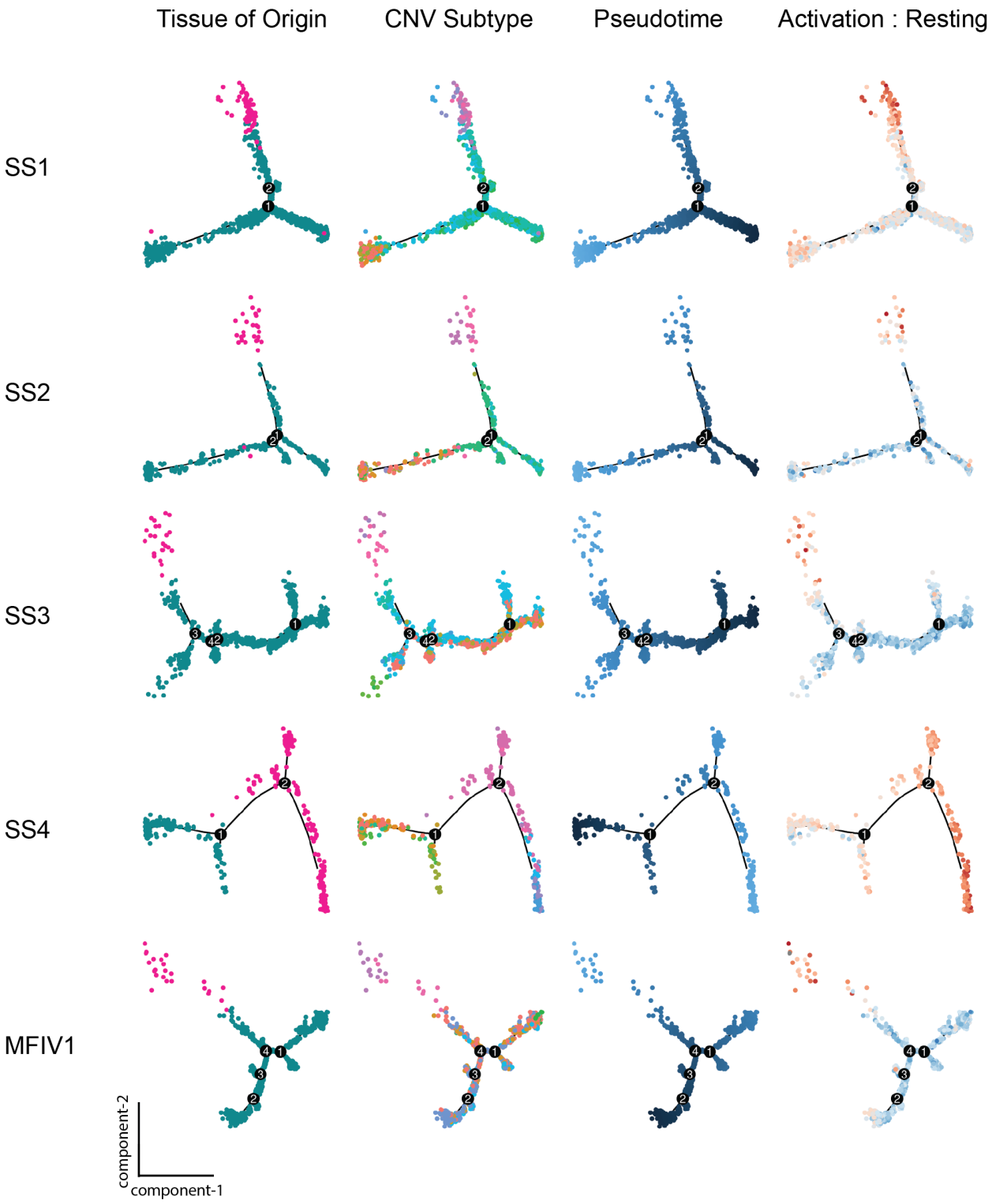

Supplementary Figure 11: Pseudotime transcriptional trajectories of malignant T cells from skin and blood of CTCL patients. Monocle-2 transcriptional trajectory analysis of

malignant T cells from the skin and blood of five CTCL patients (SS1-MFIV1) visualized based on tissue of origin, CNV-defined sub-clones, pseudotime values (earliest to latest in transcriptional projection) and activation to resting gene set ratio score. Rooting of pseudotime trajectories was set based on the CNV clones that had the shortest branch length in the phylograms.

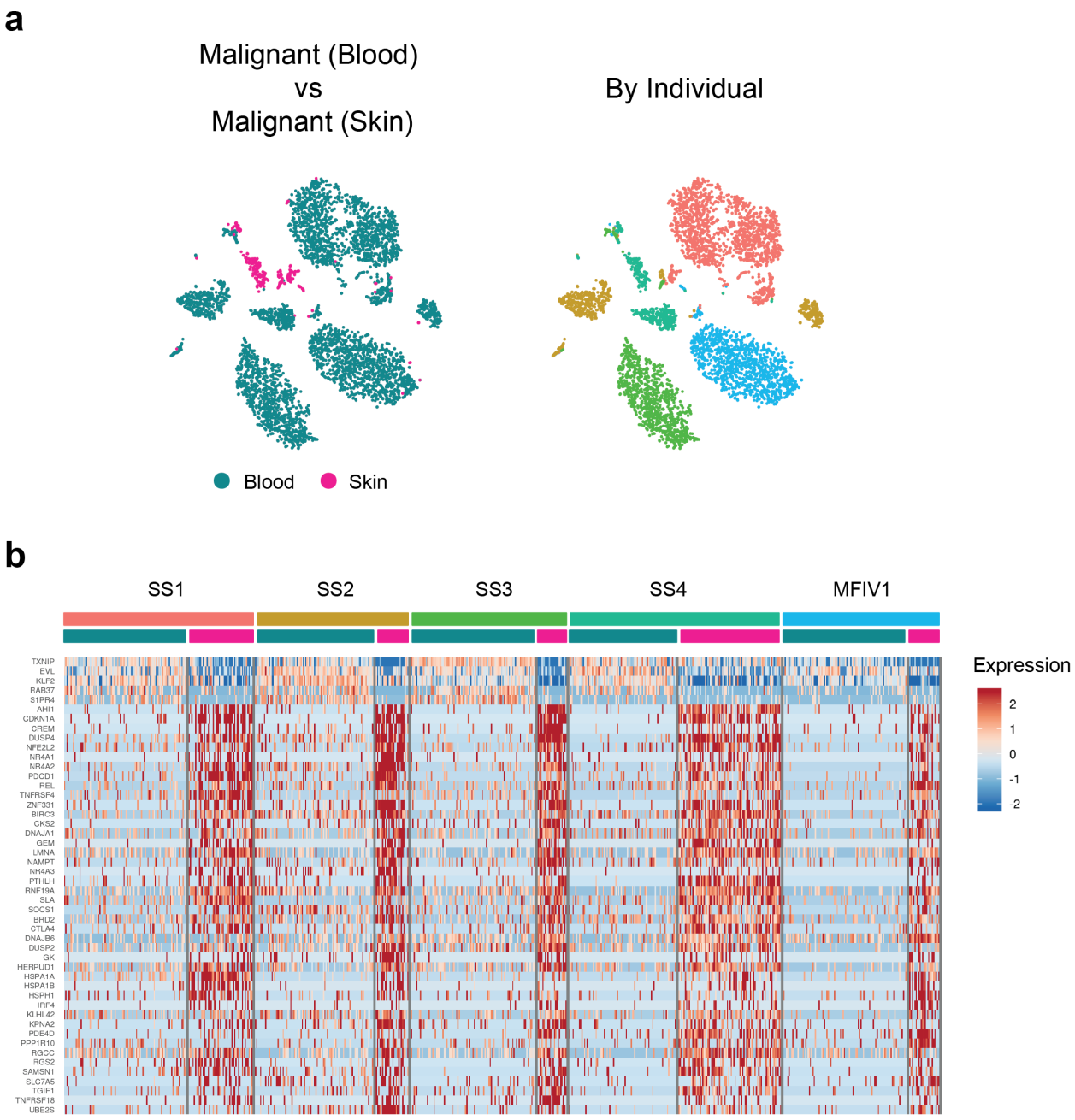

Supplementary Figure 12: Differential gene expression comparisons of paired skin- and blood-derived malignant T cells. a, t-SNE of all skin- and blood-derived malignant T cells colored by their tissue of origin (left) or individual (right) **b,** Paired comparisons between skin and blood derived malignant T cells were done independently for each of the five CTCL patients. A list of differentially expressed genes (adj p-val < 0.05, $|\log_2 FC| >= 1$) common between at least

two out of five CTCL patients was used. To mitigate over-plotting because of the blood-skin imbalance, a maximum of 100 cells from each sample was sampled out, and then ordered by patient ID to plot the heatmap.

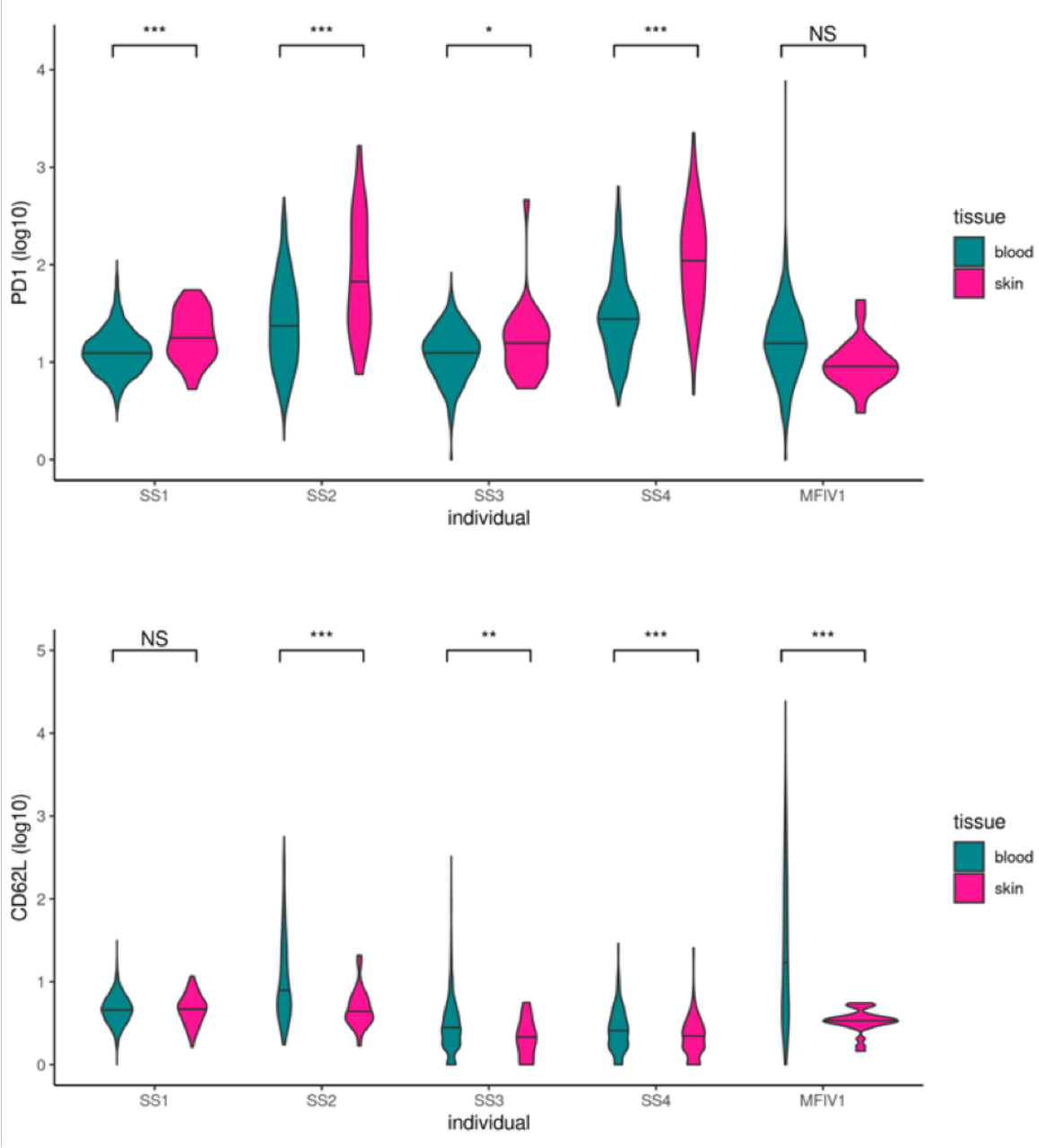

Supplementary Figure 13: Levels of surface PD-1 and CD62L expression in malignant T cells from the skin and blood of 5 CTCL patients. Violin plots showing differences in the expression of surface markers PD-1 (top) and CD62L (bottom) from skin- and blood-derived malignant T cells of five CTCL patients. Welch's two-sample t-test was used. Solid lines represent the median values and statistical significance is represented as: not significant (NS) = $p > 0.05$, * = $p < 0.05$, ** = $p < 0.01$ and *** = $p < 0.001$.

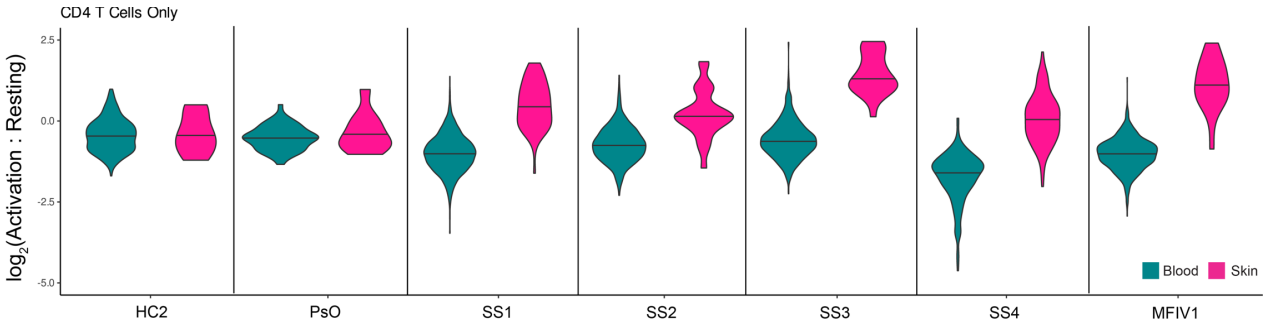

Supplementary Figure 14: Validation of enriched activation to resting transcriptional signature score ratio in skin derived T cells from CTCL patients. We compared the activation to resting score ratios in CD4+ T cells from the lesional skin and blood of 4 patients with SS and one MF stage IV patient to those from the non-lesional skin and blood of a psoriasis patient and a healthy control. Skin dissociated cells and peripheral blood PBMCs were isolated, banked and thawed identically before the ECCITE-seq protocol was run in all the samples shown.

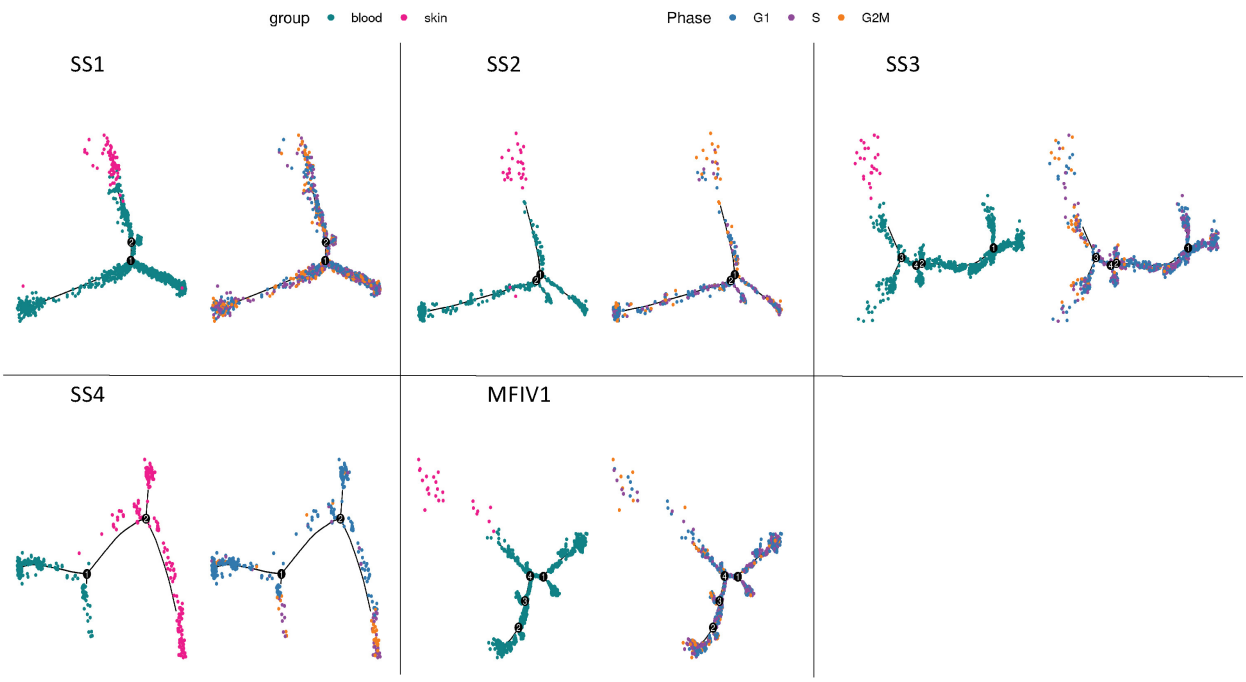

Supplementary Figure 15. Cell cycle phase analysis of malignant T cells from the skin and blood of CTCL patients. Transcriptional trajectories of skin- and blood-derived malignant T cells from five CTCL patients colored by tissue identity (left) and cell cycle phase scoring (right). Highly proliferative malignant T cells are highlighted in orange and assigned as "G2M" (G/M phases) cells.

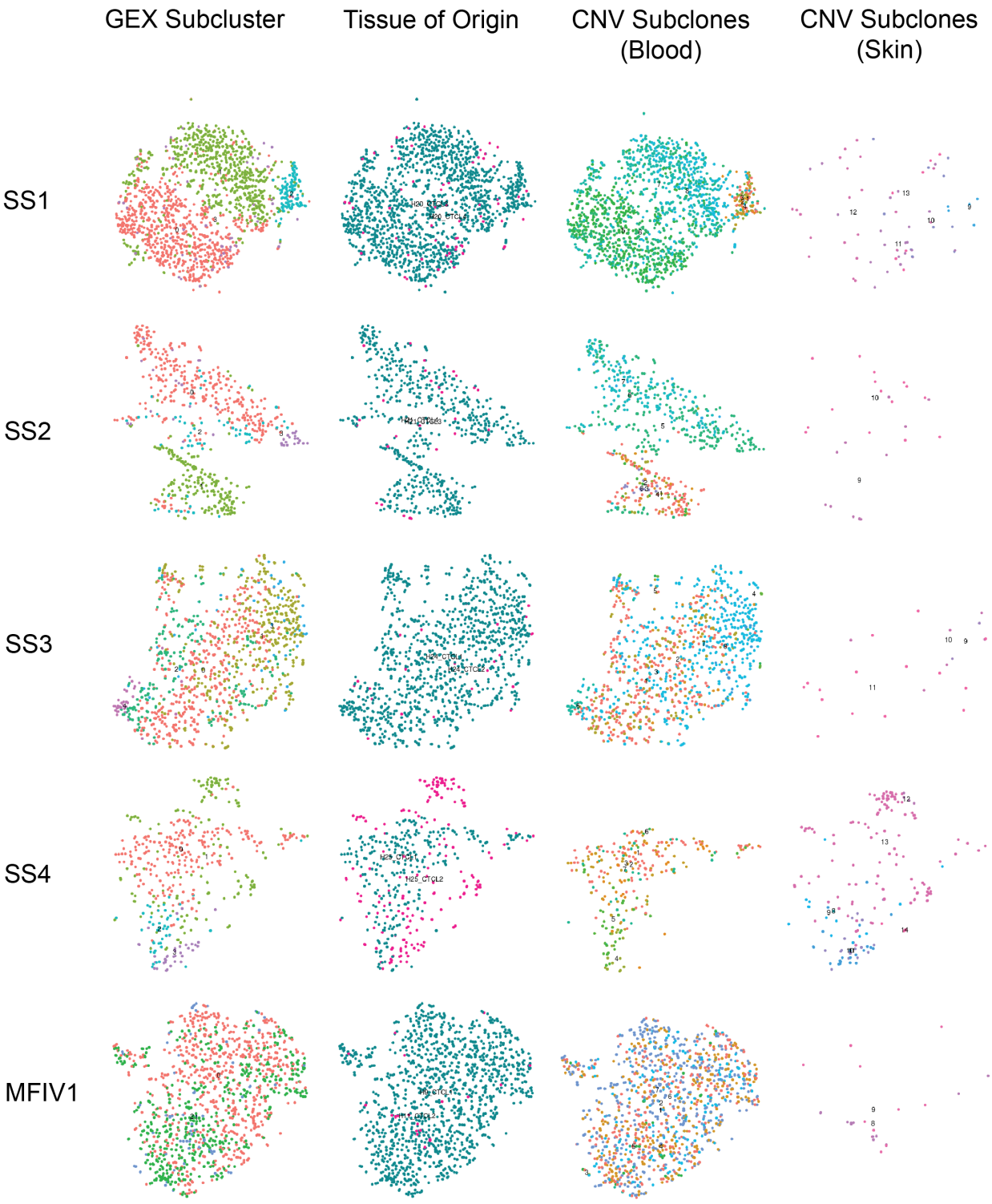

Supplementary Figure 16: Regression of tissue-based transcriptional differences between skin- and blood-derived malignant T cells. GEX-based t-SNE plots after regression

of tissue-based transcriptional differences between malignant T cells allows skin-derived malignant T cells to re-cluster heterogeneously (1st and 2nd columns; left to right). This reveals the approximate position of skin-derived malignant T cells relative to the blood-derived malignant T cell CNV sub-clones in columns 3 and 4 (left to right).

Supplementary Figure 17: Differential gene expression analysis between malignant T cells from CTCL patients. a, t-SNE plots of all blood-derived CD4+ polyclonal and

malignant T cells from seven CTCL patients clustered based on GEX. The plots are colored by presence of malignant clonality (left), by individual patient ID (middle) and by individual patient malignant clonality (right). **b,** Heatmap showing differentially expressed genes among malignant T cells from the circulation of seven CTCL patients as well as polyclonal CD4+ and CD45RO+ (memory) T cells from each patient and a healthy control.

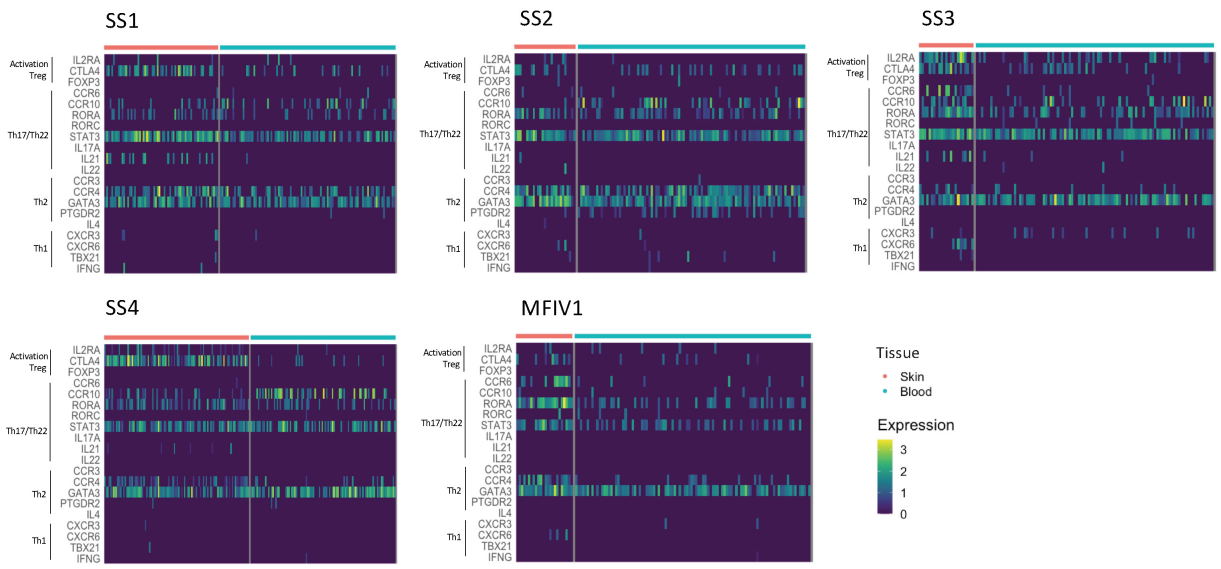

Supplementary Figure 18. Expression of characteristic T-regulatory and T-helper subtype transcripts in malignant T cells from the skin and blood of CTCL patients.

Heatmaps showing gene expression of selected transcripts (surfaces markers, transcription factors, and cytokines) associated with differentiation status of CD4+ T cells in the skin (red) and blood (blue) of five CTCL patients.

Supplementary references

1. Talevich E, Shain AH, Botton T, Bastian BC. CNVkit: Genome-Wide Copy Number Detection and Visualization from Targeted DNA Sequencing. *PLoS Comput Biol*. 2016;12(4):e1004873.
2. Gao R, Bai S, Henderson YC, et al. Delineating copy number and clonal substructure in human tumors from single-cell transcriptomes. *Nat Biotechnol*. 2021.
3. Tirosh I, Izar B, Prakadan SM, et al. Dissecting the multicellular ecosystem of metastatic melanoma by single-cell RNA-seq. *Science*. 2016;352(6282):189-196.
4. Qiu X, Mao Q, Tang Y, et al. Reversed graph embedding resolves complex single-cell trajectories. *Nat Methods*. 2017;14(10):979-982.